2017

Seasonal soil moisture and drought occurrence in Europe in CMIP5 projections for the 21st century

Ruosteenoja Kimmo

Springer Nature

Tieteelliset aikakauslehtiartikkelit

http://dx.doi.org/10.1007/s00382-017-3671-4

https://erepo.uef.fi/handle/123456789/6585

Climate Dynamics manuscript No.
(will be inserted by the editor)

Seasonal soil moisture and drought occurrence in Europe in CMIP5 projections for the 21st century

Kimmo Ruosteenoja · Tiina Markkanen · Ari Venäläinen · Petri Räisänen · Heli Peltola

Received: date / Accepted: date

Abstract Projections for near-surface soil moisture content in Europe for the 21st century were derived from simulations performed with 26 CMIP5 global climate models (GCMs). Two Representative Concentration Pathways, RCP4.5 and RCP8.5, were considered. Unlike in previous research in general, projections were calculated separately for all four calendar seasons. To make the moisture contents simulated by the various GCMs commensurate, the moisture data were normalized by the corresponding local maxima found in the output of each individual GCM. A majority of the GCMs proved to perform satisfactorily in simulating the geographical distribution of recent soil moisture in the warm season, the spatial correlation with an satellite-derived estimate varying between 0.4–0.8.

In southern Europe, long-term mean soil moisture is projected to decline substantially in all seasons. In summer and autumn, pronounced soil drying also afflicts western and central Europe. In northern Europe, drying mainly occurs in spring, in correspondence with an earlier melt of snow and soil frost. The spatial pattern of drying is qualitatively similar for both RCP scenarios, but weaker in magnitude under RCP4.5. In general, those GCMs that simulate the largest decreases in precipitation and increases in temperature and solar radiation tend to produce the most severe soil drying.

Concurrently with the reduction of time-mean soil moisture, episodes with an anomalously low soil moisture, occurring once in 10 years in the recent past simulations, become far more common. In southern Europe by the late 21st century under RCP8.5, such events would be experienced about every second year.

Keywords Near-surface soil moisture · CMIP5 GCMs · Representative Concentration Pathways (RCPs) · Climate change · Model validation

1 Introduction

During the ongoing century, precipitation is anticipated to increase in northern Europe and to decrease in the south; in central Europe, an increase is projected for winter and a decrease for summer (IPCC, 2013).

Kimmo Ruosteenoja
Finnish Meteorological Institute
P.O.Box 503, FIN-00101 Helsinki, FINLAND
Fax: +358-9-295392303
E-mail: kimmo.ruosteenoja@fmi.fi

Tiina Markkanen
Finnish Meteorological Institute

Ari Venäläinen
Finnish Meteorological Institute

Petri Räisänen
Finnish Meteorological Institute

Heli Peltola
School of Forest Sciences, University of Eastern Finland

Simultaneously, higher temperatures lead to an universal increase in potential evapotranspiration (Feng and Fu, 2013). The objective of the present work is to examine on a seasonal level how near-surface soil moisture in Europe responds to forthcoming anthropogenic climatic changes. Soil moisture changes are inferred from global climate model (GCM) simulations performed within the context of Phase 5 of the Coupled Model Intercomparison Project (CMIP5).

Examination of future changes in soil moisture constitutes a multi-disciplinary research subject that has, in addition to climatology, connections with hydrology, ecophysiology, forestry, agriculture, etc. (Seneviratne et al, 2010). In particular, soil moisture content determines how the energy from net surface radiation is partitioned into the latent heat of evapotranspiration and the flux of sensible heat into the atmosphere. Low soil moisture cuts down evapotranspiration and acts to enhance sensible heat flux, thus favouring the occurrence of high air temperatures. High temperatures in turn increase the water vapour deficit and evaporative demand in the air. This contributes to maintain evapotranspiration despite a progressive decline of soil moisture content. The influence of precipitation anomalies tends to persist in the state of soil moisture for a long time, and temporal variations in soil moisture thus engender long-term memory in the climate system.

In comparing the future temperature responses in model simulations in which soil moisture was constrained to represent either the current or future climate, Seneviratne et al (2013) concluded that the feedback induced by soil drying explained nearly 20 % of the mean temperature increase projected for southern Europe. In high temperature extremes, the contribution of soil drying proved to be even larger. In addition, a widespread drying of soil will reduce precipitation in southern Europe. Furthermore, by raising temperatures and impeding evapotranspiration, low soil moisture acts to reduce relative humidity in the lower atmosphere (Rowell and Jones, 2006).

Soil moisture content determines how tightly water is bound in the soil texture. The larger the moisture deficit in the root layer, the more negative is the soil moisture potential against which water must be extracted by the plants (Seneviratne et al, 2010). Low soil moisture leads to a stomatal closure in plants, thus reducing the ability of plants to absorb carbon dioxide for photosynthesis from the atmosphere. Because the shallowness of the root layer makes many farmed crops highly susceptible to drought, soil moisture is a key factor for the conditions of agricultural production. Accordingly, in several previous studies (e.g., Trenberth et al, 2014) moisture deficit in the root zone is termed 'agricultural drought'.

In recent years, drought stress induced by an excessively low soil moisture has been noticed to limit the regeneration success and growth of tree stands. During hot summer months with low precipitation, the mortality of trees has been observed to increase; the problem is most severe in southern Europe, but also concerns the central and northern parts of the continent (Allen et al, 2010; Lindner et al, 2010). Mortality is related to drought in the top layer of the soil where the majority of roots reside, especially in young trees (Kurjak et al, 2012). A deficit in soil moisture may also weaken the trees and thus increase various risks like insect pest damages (e.g., by bark beetle species), which most seriously threatens shallow-rooted tree species like Norway spruce (Picea abies) (Lindner et al, 2010). Moreover, dry conditions enhance the risk of devastating forest fires, particularly in southern Europe (Moriondo et al, 2006). Recently, increasing fire risks have also been projected for northern Europe (Lehtonen et al, 2016).

Ground-based in situ observations of soil moisture are available sparsely, since measurements require plenty of man-power and are therefore expensive to perform (Seneviratne et al, 2010). The records are commonly too short to yield statistically robust climatological trends. A better spatial coverage is acquired by passive and active microwave measurements from satellites, but at the expense of absolute accuracy, and the remote sensing data depict conditions in the top-most surface layer alone (Liu et al, 2012). As an alternative approach for assessing recent soil moisture trends, one can apply soil moisture models forced by meteorological data derived from observations or reanalyses (e.g., Trnka et al, 2015; Cheng et al, 2015; Gao et al, 2016; Mueller and Zhang, 2016). By combining long-term soil moisture measurements performed at a single station with soil model simulations encompassing the entire country, Trnka et al (2015) discovered a drying trend in late spring and early summer soil moisture in Czechia during the period 1961–2012.

Owing to the scarcity of reliable long-term measurement data, trends in soil moisture have frequently been assessed by examining diverse drought indices. For example, Dai (2011, 2013) explored past trends in soil moisture by applying a self-calibrated version of the Palmer Drought Severity Index (PDSI) that emulates the temporal evolution of soil moisture as a function of precipitation and potential evapotranspiration. A negative trend in PDSI was reported for southern and central Europe for the period 1950–2010, although the contribution of natural variations in soil moisture changes appeared to be large. Correspondingly, by examining the Canadian Fire Weather Index that likewise includes an estimate for soil moisture, Venäläinen et al (2014) established a drying trend for southern and eastern Europe for the period 1980–2012. According

to the Köppen classification, shifts towards dryer climate zones have likewise occurred in many areas of southern Europe (Jylhä et al, 2010). The areas affected by aridity have expanded even globally; this has been shown, for instance, by Feng and Fu (2013) and Huang et al (2016a,b) by studying observational changes in the aridity index (the ratio of annual precipitation to potential evaporation).

Regarding model projections for the future, the annually averaged moisture content of the top 10 cm soil layer has been reported to decline over the entire European continent (Dai, 2013; IPCC, 2013; Zhao and Dai, 2015). Conversely, the whole soil column considered in the models has been projected to become drier mainly in southern and central Europe, both when examining annual means (Orlowsky and Seneviratne, 2013) and the summer months only (Seneviratne et al, 2013). Furthermore, future southern European drying is apparent in hydrological quantities other than soil moisture, such as discharge (Schewe et al, 2014), the total runoff (Zhao and Dai, 2015), the ratio of precipitation to potential evaporation (Feng and Fu, 2013; Huang et al, 2016b) and the need for irrigation water in agriculture (Boehlert et al, 2015).

Soil moisture projections have been elaborated for other continents as well. For example, when studying the mean of the simulations performed with 20 CMIP5 GCMs, Cheng et al (2015) reported a decreasing future trend in annual-mean near-surface soil moisture for eastern Asia. A majority of the CMIP5 GCMs likewise simulate soil drying for North America, for nearly the whole continent in summer and everywhere apart from the arctic regions in spring (Dirmeyer et al, 2013).

In assessing future changes in soil moisture, most papers have explored either annual means (e.g., Dai, 2013; IPCC, 2013; Cheng et al, 2015; Zhao and Dai, 2015) or a single season only (e.g., Seneviratne et al, 2013). In the present work, by contrast, we examine future moisture conditions in the near-surface soil layer in Europe separately during all four calendar seasons; as will be seen below, the response of soil moisture to global warming is strongly seasonally dependent. Projections are elaborated separately for two Representative Concentration Pathway (RCP) scenarios, the RCP4.5 scenario representing moderate and RCP8.5 high greenhouse gas emissions (van Vuuren et al, 2011).

First, we introduce the GCM simulations analyzed (section 2) and validate the model simulations by comparing modelled near-surface soil moisture content with its counterpart derived from satellite microwave measurements (section 3). Subsequently, in section 4 temporally averaged soil moisture changes, relative to the baseline period 1971–2000, are shown on seasonal and monthly levels. In addition, we scrutinize soil moisture projections simulated by the individual GCMs and compare them with the corresponding changes simulated for precipitation, temperature and incident solar radiation (section 5). This analysis offers a deeper insight into the physical background of soil moisture changes and provides a complementary perspective in comparison with previous research that has focussed on the dependencies between changes in soil moisture and the components of surface energy or water balance (e.g., Seneviratne et al, 2013; Dirmeyer et al, 2013; Zhao and Dai, 2015). Finally, in section 6, we explore future changes in the frequency of episodes with an anomalously low soil moisture, i.e., incidents with soil moisture falling below the 10 year return level inferred from the the recent past simulations. As is generally known (e.g., Trenberth et al, 2014; Zhao and Dai, 2015), even a modest reduction in the temporally-averaged moisture tends to translate into large increases in the incidence of such anomalously dry epochs.

2 Climate models and verification data

In this section, the processing of the model output data is described quite briefly. A more detailed documentation is provided in the Appendix. Soil moisture projections were derived from the monthly-averaged output of the 26 GCMs listed in Table 1. We examined a historical period from 1961 to 2005 and a scenario period from 2006 to 2099; these time intervals were covered by all the model runs considered. The variable explored was the moisture content of the uppermost 10 cm layer, denoted by the acronym MRSOS.

The overall magnitude of MRSOS exhibited substantial spatial and inter-model variations. To make the soil moisture data produced by the various GCMs commensurate, the monthly mean values of MRSOS were normalized by their local maximum values found in the model output time series, determined separately for every model. The resulting normalized variable $MRSOS^{norm}$, hereafter simply termed near-surface soil moisture, invariably takes values between 0 and 100 %.

Four GCMs examined in this study (MPI-ESM-LR, MPI-ESM-MR, CMCC-CM and CMCC-CMS) did not provide data for MRSOS but solely for the entire-column moisture MRSO. These models employ a bucket scheme in soil modelling; only one grid-point value is given for soil moisture, representing the entire soil column (Roeckner et al, 2003). In these GCMs, the soil water storage capacity of the column was fairly low compared to the majority of the remaining GCMs. Applying the normalization procedure, we were

able to include these four GCMs in our analysis. As will be shown below, the future soil moisture response simulated by these GCMs did not systematically differ from that produced by the other models.

For validation of the model output, we used the observational dataset documented in Liu et al (2011, 2012). In compiling this dataset, passive and active microwave measurements were applied in conjunction with a soil model forced by atmospheric analysis fields. By considering the entire calendar years alone, the dataset covers the period 1979–2013, although the spatial and temporal coverage of the measurements is better for the later than the earlier part of that interval. The variable provided in the dataset is volumetric soil moisture in a thin (a few centimeter) surface layer. The observational moisture data were normalized in a similar manner as the GCM output data above. Although the time interval of the measurements was shorter than that covered by the GCM simulations, at least one quite a wet month was included in the observational time series nearly everywhere within the domain. Accordingly, in general the maximum values could be used as a reasonable surrogate for the field capacity, which is a prerequisite for the application of the normalization procedure.

In summer, the spatial distribution of temporally-averaged observational soil moisture appears plausible, with the largest values occurring in the cool and precipitation-rich areas of northern Europe and central European mountains and low values in the south. The distribution is qualitatively similar both for the normalized (Fig. 1(a)) and the original non-normalized (not shown) moisture variable. In the cold season when there is snow and soil frost in wide areas of Europe, the satellite measurement system does not work soundly (Liu et al, 2011, 2012). We therefore assess the performance of the GCMs in simulating near-surface soil moisture only in the warm season.

The satellite data were represented on a 0.25° latitude-longitude grid. For further analyses, the model output data, originally given on the native grids of each individual GCM, were regridded onto the same 0.25° grid by employing the nearest-neighbour method. This method was selected to avoid problems in the interpolation in coastal areas.

3 Validation of modelled soil moisture

The spatial correlations and root-mean-square (rms) differences between the observational and modelled June-September mean near-surface soil moisture fields for the period 1979–2005, calculated over the entire domain (land areas between 35–72°N, 10°W–60°E), are shown in Table 1. For the majority of the GCMs, the correlation falls between 0.4 and 0.8. Somewhat lower correlations of 0.2 to 0.4 are obtained for five GCMs (MIROC5, GFDL-CM3, GFDL-ESM2M, GISS-E2-H and GISS-E2-R). The rms differences vary between 14 and 27 percentage points, with the exception of CanESM2 for which the difference is 35 percentage points.

The corresponding validation statistics were also calculated for the multi-model mean soil moisture field. The resulting rms difference is 12 percentage points, i.e., better than what is obtained for any individual GCM (Table 1). The correlation between the observational and GCM ensemble-mean moisture distribution is 0.75, which is close to the correlation coefficient produced by the best-performing GCMs. Fig. 1(b) reveals that in summer, the ensemble-mean near-surface soil moisture simulated by the GCMs generally increases from the south to the north, and in mountain areas soil is more humid than in their adjacent low-lying areas. These features largely agree with the corresponding observational distribution (Fig. 1(a)), although in the GCM ensemble mean the fine-scale geographical details remain unresolved.

For the remaining months of the year, the correlations between the GCM-simulated and observational soil moisture distributions were generally far lower than for summer and early autumn. From December to April, even negative correlations occurred; during that season, however, the satellite data are unsuitable for any model validation (section 2).

Besides studying the long-term means, we also made an effort to compare modelled recent-past trends with their observational counterparts. Unfortunately, the soil moisture trends derived from the satellite dataset were very noisy and, over most of Europe, not statistically significant. Moreover, before 1991 the satellite data were exclusively founded on passive microwave measurements and, after that, both on passive and active measurements (Liu et al, 2011, 2012); this makes the homogeneity of the time series somewhat questionable.

In interpreting the present comparison between the GCM output and the satellite data, several caveats should be considered (Liu et al, 2011, 2012). First, the quality of the satellite data is low in the areas of frost, snow and abundant vegetation. Second, the temporal and spatial coverage of the measurements is limited, particularly during the early years of the measurement period. Third, the satellite measurements

represent the moisture content in quite a shallow (a few centimeter) layer near the surface, and moisture is given in different units than in the GCM output. The impact of this disparity is partially addressed by the normalization of both moisture variables, but consequently, it is primarily the spatial distribution rather than the absolute level of soil moisture that is validated.

We emphasize that biases in the modelled soil moisture are not always primarily caused by deficiencies in the GCM soil and land surface schemes. Rather, systematic errors in the simulated precipitation and the other atmosphere-originating forcing factors may be of larger importance (IPCC, 2013, p. 791).

Referring to the diverse shortcomings in the satellite data, Orlowsky and Seneviratne (2013) regarded that dataset as inadequate for model validation. In the present work, however, the conditions for such a comparison are somewhat more favourable since we focus on modelled soil moisture in the near-surface layer rather than in the entire soil column that was examined by Orlowsky and Seneviratne (2013). Even so, the present comparison is inherently tentative and does not permit any final and undisputed inferences about the performance of the individual GCMs. In particular, the quality of satellite data allowed model validation only for the warm season. Therefore, as well as in order to produce statistically robust multi-model mean responses, we mainly base our projections on the entire ensemble of 26 GCMs. For a sensitivity assessment, however, some analyses have been repeated by discarding those six models that received the lowest ranking in the validation (the spatial correlation with the observation-based distribution lower than 0.4 or the rms difference larger than 30 percentage points).

4 Long-term mean projections of near-surface soil moisture

Multi-model means of simulated seasonal changes in near-surface soil moisture under RCP8.5 for the period 2070–2099, relative to 1971–2000, are displayed in Fig. 2. To elucidate the robustness of the response, areas where 23 or more GCMs out of 26 agree on the direction of change are stippled.

The GCMs strongly agree on a substantial future decrease of soil moisture in southern Europe throughout the year (Fig. 2). Negative trends in soil moisture are likewise projected for central Europe, although in winter and spring the signal is weaker than in the other seasons. The areas of the most pronounced soil drying coincide with those of the largest projected reduction in the relative humidity of near-surface air (Ruosteenoja and Räisänen, 2013), indicative of a coupling between moisture conditions in the soil and atmosphere. In wide areas of northern Europe, the tendency towards drier soil conditions is less evident than elsewhere, apart from spring. In comparing the multi-model mean responses calculated for both RCP scenarios and for three 30-year future periods (Figs. S1–S4 in the electronic online resource), the geographical distribution is qualitatively similar in all cases, with the amplitude of the response becoming larger as a function of increasing greenhouse gas forcing. Moreover, the geographical patterns of the change proved to be essentially similar regardless of whether all 26 GCMs or only the 20 best-performing GCMs were included in the analysis (see section 3), although the southern European drying was slightly more pronounced in the simulations of the well-performing GCMs (Fig. S5). Also, the responses produced by those four GCMs that use the bucket scheme in soil modelling (Fig. S6) were not basically different from the 26-GCM mean response, albeit the pattern was fairly noisy. Admittedly, those four GCMs tend to simulate somewhat wetter future conditions for the north year-round and a more intense drying for central Europe in autumn, compared to the entire ensemble of GCMs.

In Fig. 2, the robustness of the multi-model mean response was inferred from the agreement of the sign of change among the GCMs. For comparison, we assessed the significance of the response by using the standard t test (Fig. S7). The area of 1 % significance proved to be even wider than the area of the high model agreement shown in Fig. 2, encompassing nearly the entire continent in summer. However, the outcome of the t test should not be interpreted quite literally as all of the 26 GCMs are not mutually independent. For example, similar parameterization methods have been used in several models and some models also share common sections of code (Pennell and Reichler, 2011).

The seasonal behaviour of the projected soil moisture trend was studied more closely by dividing Europe into six sub-regions: northern Europe covering the area to the north of 54°N, western and eastern Europe from 45°N to 54°N and the western and eastern Mediterranean regions to the south of 45°N, with the boundary between the eastern and western sub-regions at 18°E (Fig. 3). In the east, only the areas up to 50°E were included, in order to exclude the desert areas east of the Caspian Sea. The British Isles constitute a separate sub-region.

The annual course of the projected change, averaged spatially over each sub-region, is shown in Fig. 4. The seasonal distribution of drying is very similar for all three 30-year spans, with the intensity of drying

increasing monotonically as a function of time. In western Europe and the British Isles, the most pronounced drying takes place in late summer, resulting from the cumulative influences of decreasing precipitation (Fig. 12.22 of IPCC, 2013) and the warming-induced increase of potential evapotranspiration over the warm season. In the two southernmost sub-regions, drying is substantial over the entire year. In the western Mediterranean area, the most intense drying occurs in early summer, in the eastern Mediterranean sub-region in spring. Presumably this behaviour can be attributed to the very low moisture content that prevails in wide areas of southern Europe and Anatolia in late summer during the baseline period (Fig. S8). This impedes major additional drying in the future.

In northern Europe, the strongest decline in soil moisture takes place in spring. More precisely, by the first 30-year period (2010–2039), drying is most intense in May, but since that period to mid- and late 21st century, in April. From mid- to late century, non-negligible drying likewise occurs in March and during the winter months. This kind of seasonal behaviour is in concordance with the diminishing soil frost and snow cover in winter and the progressively earlier spring-time snow melt in the future (Räisänen and Eklund, 2012). Analogously, in the current climate in central Europe, a positive correlation has been identified between the inter-annual variations of winter snow water equivalent and soil moisture content in the subsequent spring and early summer (Potopová et al, 2015). In summer, drying in northern Europe is fairly modest, indicating that the increasing precipitation totals (IPCC, 2013, Fig. 12.22) partially cancel the impact of intensifying potential evapotranspiration.

In eastern Europe, the seasonal cycle of drying is bimodal. The drying peak in early spring is presumably related to an earlier melt of snow, which predates the seasonal decline of soil moisture; a similar phenomenon occurred in northern Europe. Drying in late summer and early autumn is physically analogous to that occurring in that season in western Europe.

The signal-to-noise ratio of the projected seasonal change is illustrated for the most distant scenario period (2070–2099) in Fig. S9. In northern Europe and the British Isles, the multi-model mean change dominates over the inter-model scatter only in the few spring or summer months that show the strongest projected change. Conversely, in southern Europe the signal is robust throughout the year and in central Europe in all seasons apart from winter.

In absolute terms, in southern and central Europe, August is the month with the lowest soil moisture content, while in northern Europe and the British Isles, the driest month is July (not shown). In addition to the baseline period, this holds true for all three future projection periods.

5 Dependencies between changes in soil moisture, temperature, precipitation and solar radiation

The inter-model correlations (across the 26 GCMs) of the projected spatially-averaged changes in near-surface soil moisture content with corresponding changes in near-surface air temperature, precipitation and incident solar radiation are given for the above-defined six sub-regions in Table 2. As an illustration, scatter diagrams depicting these dependencies for the eastern European sub-region are shown in Fig. 5.

In summer, the relationship between the projected changes is qualitatively similar across all the sub-regions: simulated changes in soil moisture correlate positively with the precipitation responses and negatively with the temperature and irradiance responses. The physical interpretation of these dependencies is straightforward. On the one hand, precipitation serves as a source of soil moisture, while intense solar radiation and high temperatures act to strengthen evapotranspiration. Thus, a decline in precipitation and an increase in temperature and solar radiation tend to reduce soil moisture; in some GCMs, changes in these quantities are weaker, in other GCMs stronger (Fig. 5), in concordance with the inter-model correlations evident in Table 2. On the other hand, low soil moisture intensifies the sensible heat flux into the atmosphere at the expense of latent heat flux, thus favouring the occurrence of high temperatures and low air humidity and hindering the formation of clouds. Reduced cloudiness in turn acts to enhance solar radiation.

Even the models simulating minor changes in precipitation tend to project a non-negligible reduction in soil moisture for summer (Fig. 5). This is evidently caused by enhanced potential evapotranspiration induced by increases in air temperature and (in a majority of the GCMs) solar radiation. An analogous phenomenon was noticed by Scheff and Frierson (2015) when studying future changes in the precipitation to potential evaporation ratio in relation to changes in mean precipitation.

In southern Europe, the inter-model correlations in projected changes (Table 2) are of the same sign year-round (apart from precipitation in the western Mediterranean region in autumn). Elsewhere in Europe, radiative heating is weak in winter, and thus the correlations with solar radiation change are insignificant. In the north in winter, there is no correlation with changes in precipitation or temperature either. Presumably,

in most models precipitation is large enough to keep the soil quite wet in this area, both in the baseline and future climates.

Counter-intuitively, in winter in both central European sub-regions, the correlation between the soil moisture and precipitation changes is negative (Table 2; Fig. 5). In this case, however, the fundamental factor determining the modelled soil moisture trend may be the GCM soil scheme rather than future precipitation change. Fig. 6 indicates that models with a large decrease in soil moisture during the melting season (from March to April) in the baseline-period also tend to produce a substantial reduction of soil moisture from the baseline period into the future in winter. Presumably, in these GCMs the near-surface soil layer holds water effectively in a solid state but infiltrates it in a liquid form. Thereby, the negative correlation between precipitation and soil moisture changes, which manifests itself as a tendency of many models simulating a large (small) increase in precipitation to cluster in the bottom-left (top-right) corner of Fig. 6, might be purely fortuitous.

6 Anomalously low soil moisture events

6.1 Definition

Actually, it is the incidences of extremely low soil moisture rather than a reduction in the long-term mean that are most injurious to agriculture, forestry, ecosystems, etc. In assessing probabilities for anomalous soil drought episodes for the future, we did not apply any uniform threshold value for the moisture content. Rather, the criterion of drought was dependent on the modelled local climate; i.e., a month was regarded as exceptionally dry when the near-surface soil moisture content falls below the 10th percentile inferred from the frequency distribution of moisture content in the historical simulations for the years 1961–2005. The use of a regionally-varying threshold value can be justified by the adaptation of the local ecosystems to the prevailing climatic conditions. A similar approach was adopted, e.g., by Zhao and Dai (2015), although they studied the occurrence of dry epochs without seasonal segregation. The threshold values were determined separately for every GCM, grid point and calendar month, and, in order to improve the statistical robustness, by surveying all the parallel runs. As an illustration, the 26-GCM mean of the 10th percentile values calculated for the individual GCMs for July is shown in Fig. 7. The multi-model mean of the threshold values equals 30–50 % in most of Europe but 50–70 % in the northernmost parts of the continent, the British Isles and the surroundings of the Alps.

To find the events of low soil moisture for future time spans (e.g., 2070–2099), we searched, again separately for each GCM, grid point and calendar month and considering all available parallel runs, for months with soil moisture below the determined threshold values. When considering the individual GCMs and months, the sample size is rather small (30 years multiplied by the count of parallel runs) and consequently, the geographical distributions of the fraction of months below the threshold proved to be fairly noisy. Henceforth, we therefore focus on the multi-model and seasonal means of the calculated probabilities.

Note that the determination of the percentile values from the historical model runs and the calculation of the proportion of cases falling below these percentiles in the future simulations are based on the soil moisture values arranged in an ascending order rather than on their absolute values. Therefore, probabilities for the drought occurrence determined in this section are not affected by the normalization of the soil moisture data.

6.2 Occurrence of low soil moisture events in the future

Consistently with the general drying trend discovered in section 4, episodes with an exceptionally low soil moisture content will become substantially more frequent than recently (Figs. 8 and S10–S13). During 2010–2039, the simulated frequency of the dry months already exceeds 20 % in some areas, and by mid-century, the frequency locally amounts to 30–40 %. In the late 21st century under RCP8.5, in some areas of southern and central Europe, anomalously dry months are projected to occur more commonly than every second year. The areas suffering from a frequently-occurring soil moisture deficit are most widespread in summer.

In spring, months during which soil moisture is low compared to the corresponding statistical distribution in the baseline-period climate will occur fairly frequently also in northern Europe. However, these occasions do not typically imply any extreme drought in absolute terms, since during the melting season the simulated soil moisture is generally at a tolerable level, even in anomalously dry years.

In all seasons, the geographical distribution of the occurrence of dry episodes is qualitatively similar under both RCP scenarios and during all the future time spans (Figs. 8 and S10–S13). In addition, the distribution closely resembles the pattern of long-term mean drying (Fig. 2), and the areas of a high inter-model agreement on the sign of change are similar. In the southernmost part of Europe in summer, however, the drying signal is more evident when studying the occurrence of anomalously dry months. Evidently, the low soil moisture content inhibits any major decreases in the long-term means, but the frequency distribution still shifts towards drier values, strongly enhancing the proportion of months that are classified as dry according to the current standards. Thereby, the transition may have remarkable impacts on the well-being and survival of plants, since the negative soil moisture potential increases nonlinearly as a function of exacerbating soil drought (Seneviratne et al, 2010).

In addition to the events of soil moisture lower than the 10th percentile, we looked for episodes with monthly mean soil moisture falling below the absolute minimum of the period 1961–2005. In the late 21st century summers in southern Europe under RCP8.5, the annual probability of those unprecedentedly low soil moisture events would amount to 15–25 % (Fig. 9).

7 Discussion and conclusions

As a consequence of climatic changes anticipated to occur during the ongoing century, near-surface soil moisture content is projected to decrease virtually everywhere in Europe. Concurrently, episodes with soil moisture content falling exceptionally low according to the current standards will occur far more frequently than during the recent past decades. This increasingly frequent occurrence of drought episodes is in accordance with the previous findings of Sheffield and Wood (2008) (from CMIP3 GCMs) and Zhao and Dai (2015) (from a limited ensemble of CMIP5 GCMs, focussing on annual means). In our analyses, the response of soil moisture to global warming proved to be strongly seasonally dependent. Thereby, we find it essential to study moisture changes on a seasonal level rather than solely on an annual level.

In wide areas, the drying signal is robust in the sense that at least about 90 % of the 26 GCMs examined agree on a negative future trend in soil moisture, but the magnitude of change varies across the models. In summer and in southern Europe in other seasons as well, changes in the temporally-averaged soil moisture content among the various GCMs correlate positively with simulated changes in precipitation and negatively with changes in temperature and incident solar radiation.

The general drying trend in the soil and, in particular, the increasing frequency of severe drought events will entail diverse problems for farming, natural ecosystems, forestry, building infrastructure, etc. Although the thermal growing season is projected to lengthen and the growing degree days to increase (Ruosteenoja et al, 2016), the resulting benefits are likely to be largely counteracted by the reduced availability of water. This particularly holds for southern and, to somewhat lesser degree, central Europe.

The projected reduction in soil moisture content and the increase in the frequency of drought episodes need to be considered in forest management in various regions of Europe (Lindner et al, 2010). The scarcity of soil water may result in decreased growth and carbon sequestration in forests (Kellomäki et al, 2008; Allen et al, 2010; Lindner et al, 2010; Muukkonen et al, 2015). Thus, there is an increasing pressure to modify the current forest regeneration and thinning practices in multiple European regions (Lindner et al, 2010). For example, it may be necessary to use more drought-resistant tree species and genotypes in forest regeneration. Presumably, heavier and more frequent thinnings will be needed, and the time interval between the forest regeneration and the final felling should be shortened (Briceño-Elizondo et al, 2006; Lindner et al, 2014). Furthermore, consideration of increasing fire risks under a warmer and drier climate will be particularly crucial for forest management in southern Europe (Lindner et al, 2014).

The increasingly frequent occurrence of extreme soil drought episodes leads to a shrinkage and subsidence of clay soils, which may induce damages in buildings (Pritchard et al, 2015). In the future, particularly in summer, increasingly widespread areas of Europe will shift from a humid to a transitional climate regime where evapotranspiration is constrained by soil moisture rather than the availability of heat (Seneviratne et al, 2010). In that climate type, temporal variations in the partition of surface energy flux into the sensible and latent heat components are large. This intensifies fluctuations in temperature and permits the occurrence of extremely high temperatures, thus increasing the risks of heat-related human morbidity and mortality (Dong et al, 2015).

In the present work, soil moisture has been examined in rather a thin near-surface layer. In fact, the root zone of plants is generally far deeper than 10 cm, but it is evident that the moisture content of the near-surface

layer gives a reasonable qualitative picture of moisture anomalies in the entire root zone. For the occurrence of wildfires, just the near-surface soil moisture is of particular importance (Vajda et al, 2014).

It should be emphasized that, compared to soil moisture, some other measures of drought may reveal a somewhat different picture on the occurrence of dry episodes. For example, Roudier et al (2016) projected an increase in the frequency of low flows (hydrological drought) for southern and western Europe only, whereas the drought events under that definition would be mitigated over large areas of central, eastern and northern Europe. However, that study was founded on a fairly limited set of climate models.

In the GCM simulations, soil moisture content is determined by forcing through meteorological quantities such as precipitation, temperature and solar radiation as well as by the structure of the soil and evapotranspiration sub-models. In calculating the moisture content, simulation biases in these phenomena may accumulate, explaining the divergent performance of the different GCMs in simulating the recent past soil moisture distribution (section 3). Even so, in the present paper the concordance among the GCMs about the direction of future soil moisture changes turned out to be good. Also, the reasonable agreement of soil moisture changes with the projected changes in precipitation, temperature and solar radiation in the individual models lends credibility to the present findings.

Especially under unmitigated climate change, projected changes in soil moisture involve serious drought in many European regions and thus significantly affect the functioning of terrestrial ecosystems and the preconditions of agriculture and forestry. A better understanding of future seasonal changes in soil moisture and their potential impacts will promote adaptation to changing climatic conditions and thus restrict their detrimental effects on the society.

Appendix: Detailed information on the processing of model output data

The present selection of GCMs was based on the work of Luomaranta et al (2014) who examined the performance of the CMIP5 GCMs in simulating observed temperature and precipitation in Europe. These quantities serve as the main drivers of soil moisture as well. In that paper, 28 GCMs were regarded as fit for simulating European climate. In the present study, two further GCMs were excluded: the EC-EARTH model did not provide soil moisture data at all while for NCAR-CCSM4, the simulated soil moisture content diverged considerably among the available parallel runs. To enhance the robustness of the projections, we included multiple parallel runs (with a maximum count of six, see Table 1) in our analysis.

In the CMIP5 archive, data are provided for two soil moisture variables. The variable denoted by an acronym MRSO encompasses the integrated moisture content of the entire soil column simulated by the soil sub-model of the respective GCM. There is a substantial disparity in the total depth of the soil column across the climate models (IPCC, 2013, p. 1079), and accordingly, the maximum values of MRSO in the simulated time series varied by a factor of $\sim$30 among the 26 GCMs. In many models, the soil column is much deeper than the root zone of plants, and thus the lower parts of the column do not interact actively with the surface and the overlying atmosphere.

The other variable, MRSOS, depicts soil moisture content in the uppermost 10 cm layer. Thus, this quantity is more commensurate across the GCMs than MRSO. The whole root zone is not taken into account, but in a qualitative sense the temporal variations of moisture near the surface coincide moderately well with those deeper in the root zone (e.g., Hauck et al, 2011; Pei et al, 2016); abundant rainfall events or long-lasting dry periods induce moisture anomalies of the same sign in the entire root zone rather than in the near-surface layer alone. In contrast to MRSO, future changes in MRSOS proved to be strongly seasonally dependent (section 4). Note that both soil moisture variables include the total mass of water (in kgm^{-2}) in all phases, both ice and liquid water; the water content of the snow cover is not incorporated, however.

There are notable inter-model differences in the simulated temporal means of MRSOS as well, even though less dramatic than in MRSO. Moreover, individual model simulation exhibit significant spatial variations. This indicates that the water-holding capacity of the near-surface soil layer is variable. To make the moisture contents from the various models and locations commensurate, we first assumed that the local water-holding capacity can be approximated by the long-term maximum of near-surface soil moisture. To improve the robustness, these maxima were determined by going through the entire time series of model output from 1961 to 2099, and the time series were expanded by pooling both RCP scenarios, all the parallel runs and all calendar months. The resulting maximum values proved to be significantly smaller than elsewhere only in the arid regions in the Near East and central Eurasia and, in some GCMs, in areas in the immediately vicinity of the Mediterranean Sea; in the other portions of the domain, there were no systematic spatial variations. Consequently, we conclude that over the majority of the domain the maximum value of

MRSOS derived from the model output serves as a reasonable proxy for the local water-holding capacity (or the field capacity in frost-free areas) of the near-surface soil layer of each GCM.

After finding the maximum values, we determined a normalized variable representing near surface soil moisture by dividing the monthly means of MRSOS by the maxima:

$$MRSOS^{norm}_{\lambda,\phi,t,m,r} = 100\% \times MRSOS_{\lambda,\phi,t,m,r} / MRSOS^{max}_{\lambda,\phi,m} \quad (1)$$

where λ and ϕ stand for the longitude and latitude, t the time and m the climate model, and r specifies the model run (one of the historical, RCP4.5 or RCP8.5 parallel runs).

In the CNRM-CM5 model, the depth of the surface layer is 1 cm rather than 10 cm, but normalization made the MRSOS data from that model comparable to the remaining models.

Several previous studies have examined a soil moisture index that emulates the share of soil moisture available for plants, with a zero value of the index corresponding to the permanent wilting point and unity to the field capacity (see, e.g., Seneviratne et al, 2010; Gao et al, 2016, and references therein). This approach was not feasible in the present study, since in humid areas monthly mean soil moisture never reaches the wilting point.

In determining the multi-model mean changes of soil moisture (section 4), we first calculated averages over the available parallel runs for each GCM. Thereafter, these were used to calculate multi-model means by weighting all the GCMs equally. However, there is one research centre (MIROC) from which three model versions have been included in the ensemble (Table 1). In order not to overemphasize the MIROC models, halved weights were assigned to MIROC-ESM and MIROC-ESM-CHEM.

Supporting information

As a part of this article, an online resource (electronic supplement file) is available, containing Supplementary Figures S1–S13.

Acknowledgements This work has been funded by the Academy of Finland (the ADAPT and PLUMES projects, decisions 260785 and 278067, and the FORBIO project of the Strategic Research Council), the Finnish Ministry of Agriculture and Forestry (the ILMA-PUSKURI project) and the European Commission (the Life+ project MONIMET, Grant agreement LIFE12 ENV/FI000409). The CMIP5 GCM data were downloaded from the Earth System Grid Federation data archive (http://pcmdi9.llnl.gov) and the remotely-sensed soil moisture data from the Climate Change Initiative Phase 1 Soil Moisture Project of the European Space Agency (http://www.esa-cci.org/). The two unknown reviewers are thanked for constructive comments.

References

Allen C, Macalady A, Chenchouni H, Bachelet D, McDowell N, Vennetier M, Kitzberger T, Rigling A, Breshears DD, Hogg E, Gonzalez P, Fensham R, Zhang Z, Castro J, Demidova N, Lim JH, Allard G, Running SW, Semerci A, Cobb N (2010) A global overview of drought and heat-induced tree mortality reveals emerging climate change risks for forests. Forest Ecology and Management 259:660–684, DOI 10.1016/j.foreco.2009.09.001

Boehlert B, Solomon S, Strzepek KM (2015) Water under a changing and uncertain climate: Lessons from climate model ensembles. Journal of Climate 28:9561–9582, DOI 10.1175/JCLI-D-14-00793.1

Briceño-Elizondo E, Garcia-Gonzalo J, Peltola H, Matala J, Kellomäki S (2006) Sensitivity of growth of Scots pine, Norway spruce and silver birch to climate change and forest management in boreal conditions. Forest Ecology and Management 232:152–167, DOI 10.1016/j.foreco.2006.05.062

Cheng S, Guan X, Huang J, Ji F, Guo R (2015) Long-term trend and variability of soil moisture over East Asia. Journal of Geophysical Research: Atmospheres 120:8658–8670, DOI 10.1002/2015JD023206

Dai A (2011) Characteristics and trends in various forms of the Palmer Drought Severity Index during 1900–2008. Journal of Geophysical Research: Atmospheres 116:D12,115, DOI 10.1029/2010JD015541

Dai A (2013) Increasing drought under global warming in observations and models. Nature Clim Change 3:52–58, DOI 10.1038/NCLIMATE1633

Dirmeyer PA, Jin Y, Singh B, Yan X (2013) Evolving land-atmosphere interactions over North America from CMIP5 simulations. Journal of Climate 26:7313–7327, DOI 10.1175/JCLI-D-12-00454.1

Dong W, Liu Z, Liao H, Tang Q, Li X (2015) New climate and socio-economic scenarios for assessing global human health challenges due to heat risk. Climatic Change 130:505–518, DOI 10.1007/s10584-015-1372-8

Feng S, Fu Q (2013) Expansion of global drylands under a warming climate. Atmospheric Chemistry and Physics 13:10,081–10,094, DOI 10.5194/acp-13-10081-2013

Gao Y, Markkanen T, Thum T, Aurela M, Lohila A, Mammarella I, Kämäräinen M, Hagemann S, Aalto T (2016) Assessing various drought indicators in representing summer drought in boreal forests in Finland. Hydrology and Earth System Sciences 20:175–191, DOI 10.5194/hess-20-175-2016

Hauck C, Barthlott C, Krauss L, Kalthoff N (2011) Soil moisture variability and its influence on convective precipitation over complex terrain. Quarterly Journal of the Royal Meteorological Society 137:42–56, DOI 10.1002/qj.766

Huang J, Ji M, Xie Y, Wang S, He Y, Ran J (2016a) Global semi-arid climate change over last 60 years. Climate Dynamics 46:1131–1150, DOI 10.1007/s00382-015-2636-8

Huang J, Yu H, Guan X, Wang G, Guo R (2016b) Accelerated dryland expansion under climate change. Nature Climate Change 6:166–172, DOI 10.1038/nclimate2837

IPCC (2013) Climate Change 2013: The physical science basis. Contribution of Working Group I to the Fifth Assessment Report of the Intergovernmental Panel on Climate Change. Cambridge University Press, Cambridge, U.K., 1535 pp, [Stocker, T.F., D. Qin, G.-K. Plattner, M. Tignor, S.K. Allen, J. Boschung, A. Nauels, Y. Xia, V. Bex and P.M. Midgley (eds.)]

Jylhä K, Tuomenvirta H, Ruosteenoja K, Niemi-Hugaerts H, Keisu K, Karhu JA (2010) Observed and projected future shifts of climate zones in Europe and their use to visualize climate change information. Wea Climate Soc 2:148–167

Kellomäki S, Peltola H, Nuutinen T, Korhonen KT, Strandman H (2008) Sensitivity of managed boreal forests in Finland to climate change, with implications for adaptive management. Philosophical Transactions of the Royal Society B: Biological Sciences 363:2341–2351, DOI 10.1098/rstb.2007.2204

Kurjak D, Střelcová K, Ditmarová L, Priwitzer T, Kmet' J, Homolák M, Pichler V (2012) Physiological response of irrigated and non-irrigated Norway spruce trees as a consequence of drought in field conditions. Eur J For Res 131:1737–1746, DOI 10.1007/s10342-012-0611-z

Lehtonen I, Venäläinen A, Kämäräinen M, Peltola H, Gregow H (2016) Risk of large-scale fires in boreal forests of Finland under changing climate. Nat Hazards Earth Syst Sci 16:239–253, DOI 10.5194/nhess-16-239-2016

Lindner M, Maroschek M, Netherer S, Kremer A, Barbati A, Garcia-Gonzalo J, Seidl R, Delzon S, Corona P, Kolström M, Lexer MJ, Marchetti M (2010) Climate change impacts, adaptive capacity, and vulnerability of European forest ecosystems. Forest Ecology and Management 259:698–709, DOI 10.1016/j.foreco.2009.09.023

Lindner M, Fitzgerald JB, Zimmermann N, Reyer C, Delzon S, van der Maaten E, Schelhaas MJ, Lasch P, Eggers J, van der Maaten-Theunissen M, Suckow F, Psomas A, Poulter B, Hanewinkel M (2014) Climate change and European forests: What do we know, what are the uncertainties, and what are the implications for forest management? Journal of Environmental Management 146:69–83, DOI 10.1016/j.jenvman.2014.07.030

Liu Y, Dorigo W, Parinussa R, de Jeu R, Wagner W, McCabe M, Evans J, van Dijk A (2012) Trend-preserving blending of passive and active microwave soil moisture retrievals. Remote Sensing of Environment 123:280–297, DOI 10.1016/j.rse.2012.03.014

Liu YY, Parinussa RM, Dorigo WA, De Jeu RAM, Wagner W, van Dijk AIJM, McCabe MF, Evans JP (2011) Developing an improved soil moisture dataset by blending passive and active microwave satellite-based retrievals. Hydrology and Earth System Sciences 15:425–436, DOI 10.5194/hess-15-425-2011

Luomaranta A, Ruosteenoja K, Jylhä K, Gregow H, Haapala J, Laaksonen A (2014) Multimodel estimates of the changes in the Baltic Sea ice cover during the present century. Tellus A 66:22,617, DOI http://dx.doi.org/10.3402/tellusa.v66.22617

Moriondo M, Good P, Durao R, Bindi M, Giannakopoulos C, Corte-Real J (2006) Potential impact of climate change on fire risk in the Mediterranean area. Climate Research 31:85–95

Mueller B, Zhang X (2016) Causes of drying trends in northern hemispheric land areas in reconstructed soil moisture data. Climatic Change 134:255–267, DOI 10.1007/s10584-015-1499-7

Muukkonen P, Nevalainen S, Lindgren M, Peltoniemi M (2015) Spatial occurrence of drought-associated damages in Finnish boreal forests: results from forest condition monitoring and GIS analysis. Boreal Environment Research 20:172–180

Orlowsky B, Seneviratne SI (2013) Elusive drought: uncertainty in observed trends and short- and long-term CMIP5 projections. Hydrology and Earth System Sciences 17:1765–1781, DOI 10.5194/hess-17-1765-2013

Pei L, Moore N, Zhong S, Kendall AD, Gao Z, Hyndman DW (2016) Effects of irrigation on summer precipitation over the United States. Journal of Climate 29:3541–3558, DOI 10.1175/JCLI-D-15-0337.1

Pennell C, Reichler T (2011) On the effective number of climate models. J Climate 24:2358–2367, DOI 10.1175/2010JCLI3814.1

Potopová V, Boroneanţ C, Možný M, Soukup J (2015) Driving role of snow cover on soil moisture and drought development during the growing season in the Czech Republic. International Journal of Climatology 36:3741–3758, DOI 10.1002/joc.4588

Pritchard OG, Hallett SH, Farewell TS (2015) Probabilistic soil moisture projections to assess Great Britain's future clay-related subsidence hazard. Climatic Change 133:635–650, DOI 10.1007/s10584-015-1486-z

Räisänen J, Eklund J (2012) 21st century changes in snow climate in Northern Europe: a high-resolution view from ENSEMBLES regional climate models. Climate Dynamics 38:2575–2591, DOI 10.1007/s00382-011-1076-3

Roeckner E, Bäuml G, Bonaventura L, Brokopf R, Giorgetta MEM, Hagemann S, Kirchner I, Manzini LKE, Rhodin A, Schlese U, Schulzweida U, Tompkins A (2003) The atmospheric general circulation model ECHAM5. Part I: Model description. Tech. Rep. 349, Max-Planck-Institut für Meteorologie, Bundesstrasse 55 D, 20146 Hamburg, Germany

Roudier P, Andersson JCM, Donnelly C, Feyen L, Greuell W, Ludwig F (2016) Projections of future floods and hydrological droughts in Europe under a +2°C global warming. Climatic Change 135:341–355, DOI 10.1007/s10584-015-1570-4

Rowell DP, Jones RG (2006) Causes and uncertainty of future summer drying over Europe. Clim Dynam 27:281–299, DOI 10.1007/s00382-006-0125-9

Ruosteenoja K, Räisänen P (2013) Seasonal changes in solar radiation and relative humidity in Europe in response to global warming. J Climate 26:2467–2481, DOI 10.1175/JCLI-D-12-00007.1

Ruosteenoja K, Räisänen J, Venäläinen A, Kämäräinen M (2016) Projections for the duration and degree days of the thermal growing season in Europe derived from CMIP5 model output. International Journal of Climatology 36:3039–3055, DOI 10.1002/joc.4535

Scheff J, Frierson DMW (2015) Terrestrial aridity and its response to greenhouse warming across CMIP5 climate models. Journal of Climate 28:5583–5600, DOI 10.1175/JCLI-D-14-00480.1

Schewe J, Heinke J, Gerten D, Haddeland I, Arnell NW, Clark DB, Dankers R, Eisner S, Fekete BM, Colón-González FJ, Gosling SN, Kim H, Liu X, Masaki Y, Portmann FT, Satoh Y, Stacke T, Tang Q, Wada Y, Wisser D, Albrecht T, Frieler K, Piontek F, Warszawski L, Kabat P (2014) Multimodel assessment of water scarcity under climate change. Proceedings of the National Academy of Sciences 111:3245–3250, DOI 10.1073/pnas.1222460110

Seneviratne SI, Corti T, Davin EL, Hirschi M, Jaeger EB, Lehner I, Orlowsky B, Teuling AJ (2010) Investigating soil moisture-climate interactions in a changing climate: A review. Earth-Science Reviews 99:125–161, DOI 10.1016/j.earscirev.2010.02.004

Seneviratne SI, Wilhelm M, Stanelle T, van den Hurk B, Hagemann S, Berg A, Cheruy F, Higgins ME, Meier A, Brovkin V, Claussen M, Ducharne A, Dufresne JL, Findell KL, Ghattas J, Lawrence DM, Malyshev S, Rummukainen M, Smith B (2013) Impact of soil moisture-climate feedbacks on CMIP5 projections: First results from the GLACE-CMIP5 experiment. Geophysical Research Letters 40:5212–5217, DOI 10.1002/grl.50956

Sheffield J, Wood EF (2008) Projected changes in drought occurrence under future global warming from multi-model, multi-scenario, IPCC AR4 simulations. Climate Dynamics 31:79–105, DOI 10.1007/s00382-007-0340-z

Trenberth KE, Dai A, van der Schrier G, Jones PD, Barichivich J, Briffa KR, Sheffield J (2014) Global warming and changes in drought. Nature climate change 4:17–22, DOI 10.1038/NCLIMATE2067

Trnka M, Brázdil R, Možný M, Štěpánek P, Dobrovolný P, Zahradníček P, Balek J, Semerádová D, Dubrovský M, Hlavinka P, Eitzinger J, Wardlow B, Svoboda M, Hayes M, Žalud Z (2015) Soil moisture trends in the Czech Republic between 1961 and 2012. International Journal of Climatology 35:3733–3747, DOI 10.1002/joc.4242

Vajda A, Venäläinen A, Suomi I, Junila P, Mäkelä HM (2014) Assessment of forest fire danger in a boreal forest environment: description and evaluation of the operational system applied in Finland. Meteorological Applications 21:879–887, DOI 10.1002/met.1425

Venäläinen A, Korhonen N, Hyvärinen O, Koutsias N, Xystrakis F, Urbieta IR, Moreno JM (2014) Temporal variations and change in forest fire danger in Europe for 1960–2012. Natural Hazards and Earth System Sciences 14:1477–1490, DOI 10.5194/nhess-14-1477-2014

van Vuuren DP, Edmonds J, Kainuma M, Riahi K, Thomson A, Hibbard K, Hurtt GC, Kram T, Krey V, Lamarque JF, Masui T, Meinshausen M, Nakicenovic N, Smith SJ, Rose SK (2011) The representative concentration pathways: an overview. Climatic Change 109:5–31, DOI 10.1007/s10584-011-0148-z

Zhao T, Dai A (2015) The magnitude and causes of global drought changes in the twenty-first century under a low-moderate emissions scenario. Journal of Climate 28:4490–4512, DOI 10.1175/JCLI-D-14-00363.1

Table 1 Global climate models used in creating the soil moisture projections. The first and second columns state the model acronym and the country of origin. Columns 3–5 indicate the count of parallel runs that were analyzed for the historical period and for both RCP scenarios. The last two columns show the spatial correlations and rms differences (calculated over Europe and averaged from June to September) between the modelled and observation-derived temporally-averaged normalized soil moisture for the period 1979–2005. The rms differences are expressed in percentage points.

Model	Country	N_{hist}	$N_{4.5}$	$N_{8.5}$	Correl	RMS
MIROC5	Japan	4	3	3	0.37	19
MIROC-ESM	Japan	3	1	1	0.58	15
MIROC-ESM-CHEM	Japan	1	1	1	0.55	16
MRI-CGCM3	Japan	3	1	1	0.77	14
BCC-CSM1-1	China	3	1	1	0.47	19
INMCM4	Russia	1	1	1	0.60	16
NorESM1-M	Norway	3	1	1	0.56	14
NorESM1-ME	Norway	1	1	1	0.55	14
HadGEM2-ES	U.K.	5	4	4	0.77	26
HadGEM2-CC	U.K.	3	1	3	0.78	24
MPI-ESM-LR	Germany	3	3	3	0.64	16
MPI-ESM-MR	Germany	3	3	1	0.63	16
CNRM-CM5	France	6	1	5	0.47	27
IPSL-CM5A-LR	France	6	4	4	0.68	22
IPSL-CM5A-MR	France	3	1	1	0.75	22
CMCC-CM	Italy	1	1	1	0.51	17
CMCC-CMS	Italy	1	1	1	0.60	17
GFDL-CM3	U.S.A.	4	1	1	0.29	16
GFDL-ESM2M	U.S.A.	1	1	1	0.22	18
GISS-E2-R	U.S.A.	6	6	2	0.23	20
GISS-E2-H	U.S.A.	6	5	2	0.25	20
NCAR-CESM1-CAM5	U.S.A.	3	3	3	0.44	15
NCAR-CESM1-BGC	U.S.A.	1	1	1	0.47	15
CanESM2	Canada	5	5	5	0.60	35
ACCESS1-0	Australia	2	1	1	0.74	25
ACCESS1-3	Australia	3	1	1	0.74	14
Multi-model mean					0.75	12

Table 2 Inter-model correlation coefficients between projected seasonal sub-region-average changes (from 1971–2000 to 2070–2099; the RCP8.5 scenario) in near-surface soil moisture content and changes in near-surface air temperature, precipitation and incident solar radiation calculated across the model ensemble. The correlations are given separately for six European sub-regions: northern Europe, the British Isles, western and eastern Europe and western and eastern Mediterranean regions. For the geographical extent and acronyms used for the sub-regions, see Fig. 3. According to a two-tailed t test, correlations with an absolute value higher than 0.39 are statistically significant at the 5 % level (boldfaced), those higher than 0.50 at the 1 % level (nonetheless, these thresholds should be interpreted with caution as the model ensemble is not totally independent).

Region	N-EUR	BRI-IS	W-EUR	E-EUR	W-MED	E-MED
Dec–Feb						
Temperature	-0.16	0.01	**-0.49**	-0.38	**-0.50**	**-0.50**
Precipitation	0.01	0.26	**-0.49**	**-0.50**	**0.64**	0.06
Solar rad.	0.06	0.10	0.11	0.25	**-0.76**	-0.26
Mar–May						
Temperature	-0.17	0.19	-0.36	**-0.57**	**-0.74**	**-0.65**
Precipitation	-0.07	**0.48**	0.07	0.01	0.33	**0.59**
Solar rad.	-0.11	-0.11	-0.13	-0.26	**-0.63**	-0.27
Jun–Aug						
Temperature	**-0.46**	**-0.43**	**-0.63**	**-0.65**	**-0.55**	**-0.57**
Precipitation	**0.64**	**0.60**	**0.72**	**0.65**	0.28	0.29
Solar rad.	**-0.63**	-0.37	-0.36	**-0.46**	-0.21	-0.15
Sep–Nov						
Temperature	-0.18	-0.38	**-0.58**	**-0.63**	**-0.80**	**-0.70**
Precipitation	0.12	0.16	**0.42**	**0.49**	-0.10	0.36
Solar rad.	-0.22	-0.20	-0.16	-0.26	**-0.66**	**-0.57**

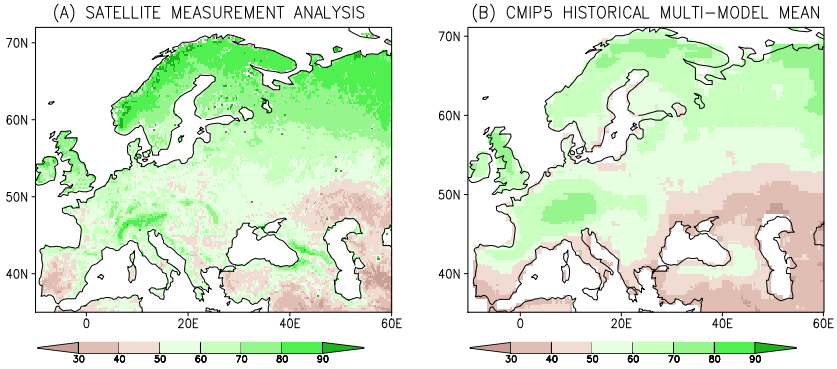

Fig. 1 Temporally averaged normalized near-surface soil moisture in June-September for the period 1979–2013 as derived from (a) the satellite analyses produced by Liu et al (2011, 2012) and (b) from the historical simulations performed with 26 CMIP5 GCMs (a multi-model mean).

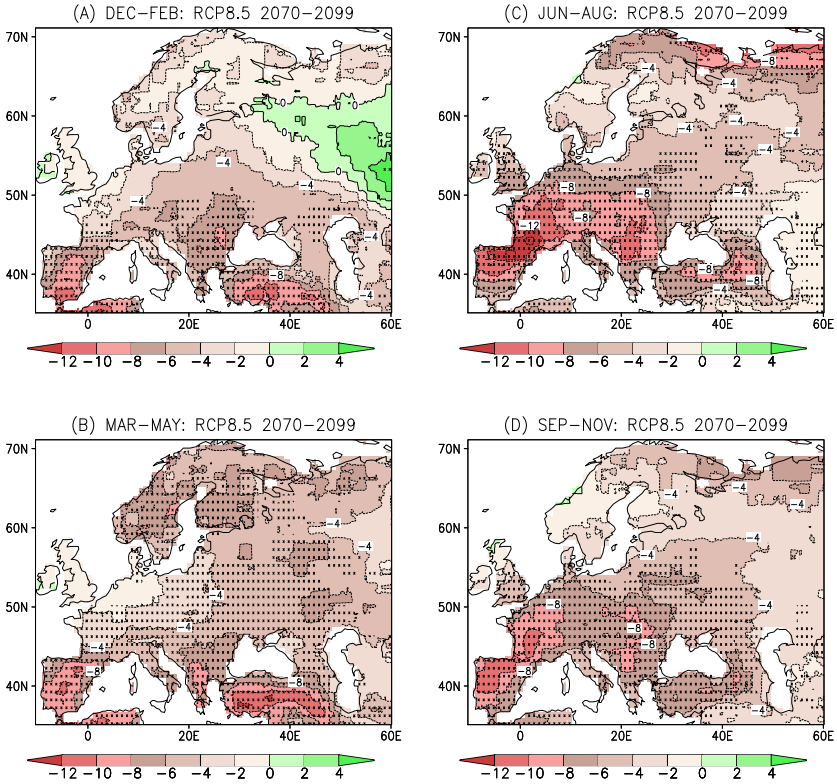

Fig. 2 Projected changes in time-mean near-surface soil moisture (in percentage points) in Europe in (a) December-February, (b) March-May, (c) June-August and (d) September-November under the RCP8.5 scenario for the period 2070–2099, relative to 1971–2000, averaged over the 26 GCMs listed in Table 1. Areas where at least 23 models agree on the sign of change are stippled.

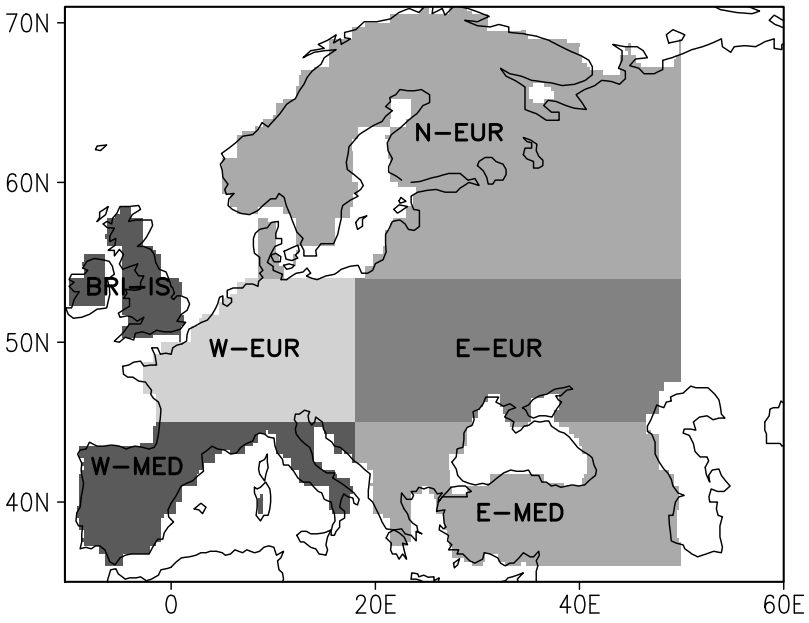

Fig. 3 The six European sub-regions used for representing the soil moisture projections: N-EUR – Northern Europe; BRI-IS – British Isles; W-EUR – Western Europe; E-EUR – Eastern Europe; W-MED – Western Mediterranean; and E-MED – Eastern Mediterranean region.

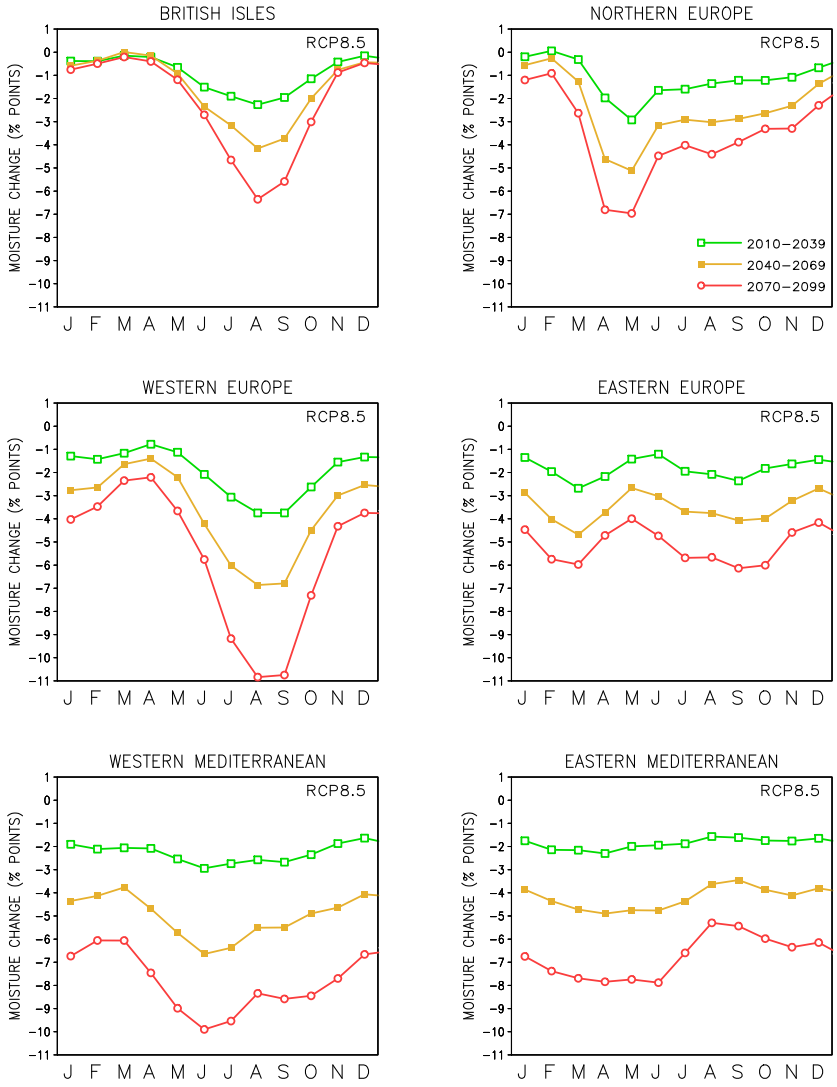

Fig. 4 Multi-model mean monthly responses (J = January, F = February, ...) in near-surface soil moisture (in percentage points) for three future time spans (2010–2039, 2040–2069 and 2070–2099, relative to 1971–2000; see the legend) under the RCP8.5 scenario; averages over the six European sub-regions depicted in Fig. 3.

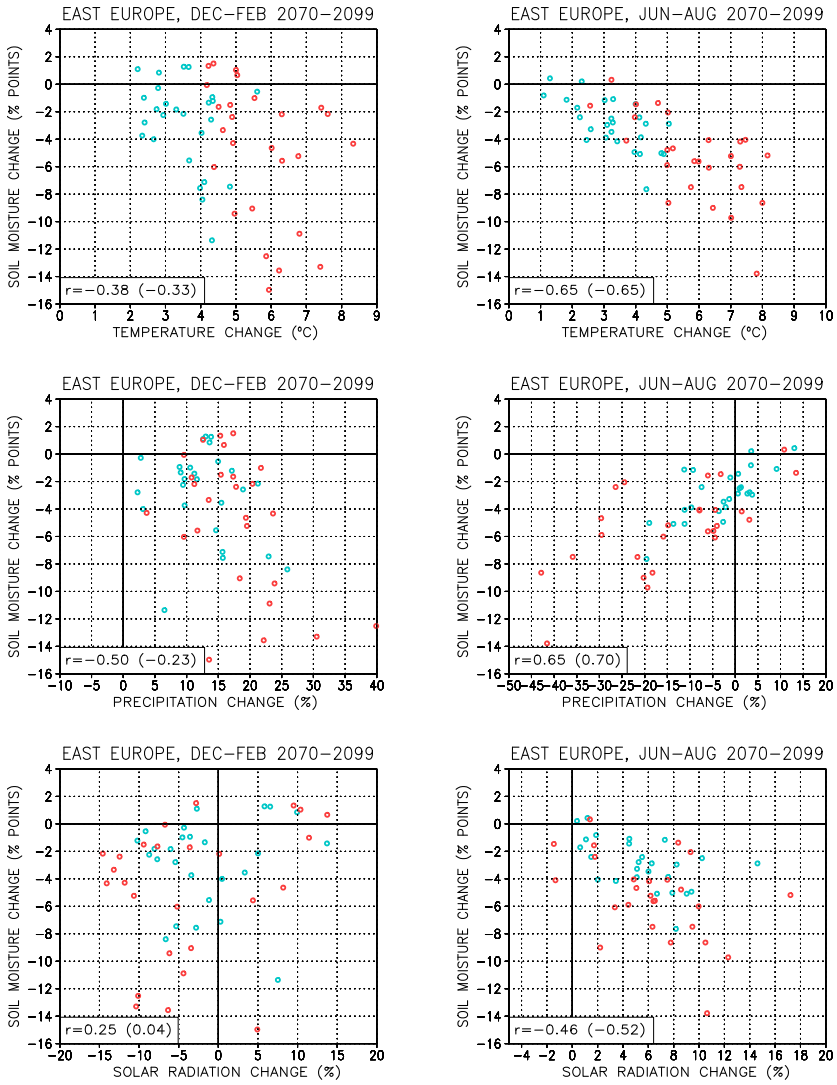

Fig. 5 Scatter diagrams showing simulated changes (from 1971–2000 to 2070–2099) in soil moisture in the individual models, in conjunction with corresponding changes in near-surface air temperature (top) precipitation (middle) and incident solar radiation (bottom); spatial averages over the Eastern European region (45–54°N, 18–50°E). The left panels depict the bivariate distributions for December-February and the right panels for June-August; model simulations under RCP4.5 are marked by blue and those under RCP8.5 by red symbols. The inter-model correlation coefficients between the responses in the two variables under RCP8.5 (in parentheses, for RCP4.5) are given in the bottom-left corner of each panel. Correlations higher than 0.39 are significant at the 5 % level, those over 0.50 at the 1 % level (24 degrees of freedom).

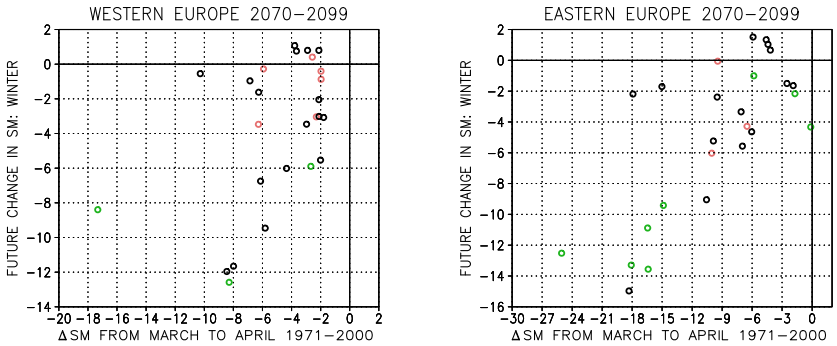

Fig. 6 Future changes in soil moisture in winter as a function of the vernal drying of the soil in the baseline climate in the individual models. Vertical axis: simulated changes in soil moisture (in percentage points) from 1971–2000 to 2070–2099 for December-February under RCP8.5. Horizontal axis: a difference between the soil moisture contents of April and March during the period 1971–2000. Models simulating an increase of less than 10 % (more than 20 %) for winter mean precipitation are marked by red (green); other models by black. Left panel: spatial mean over western Europe; right panel: eastern Europe (see Fig. 3).

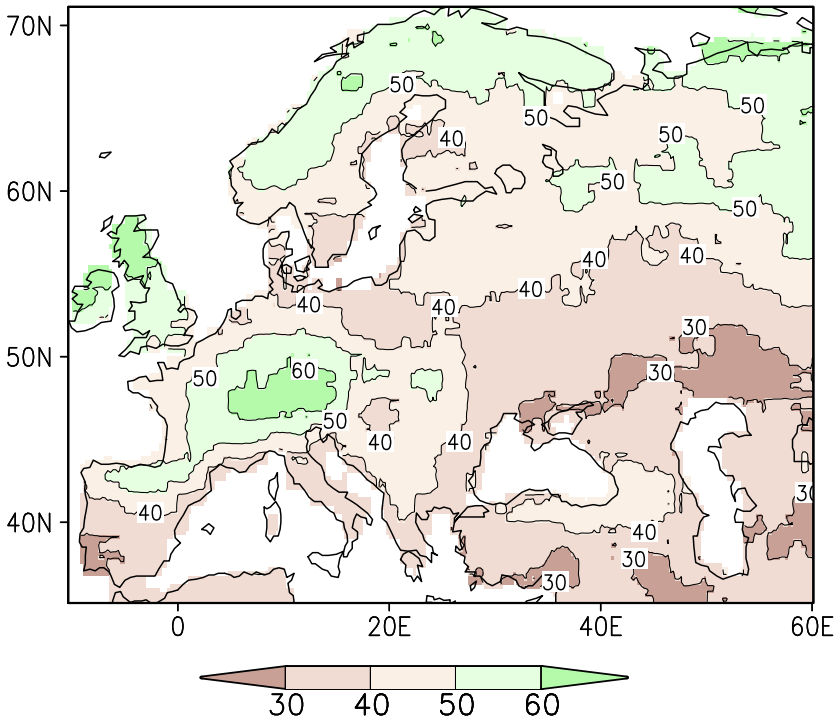

Fig. 7 Geographical pattern of the 10th percentile of normalized soil moisture in July; a multi-model mean of the percentiles calculated for the 26 GCMs from historical simulations for the years 1961–2005, considering all the parallel runs. For models providing only one parallel run, the 10th percentile is given by the 5th member of the 45 moisture values arranged in an increasing order. Correspondingly, if two parallel runs are available, the percentile is the mean of the 9th and 10th member, etc.

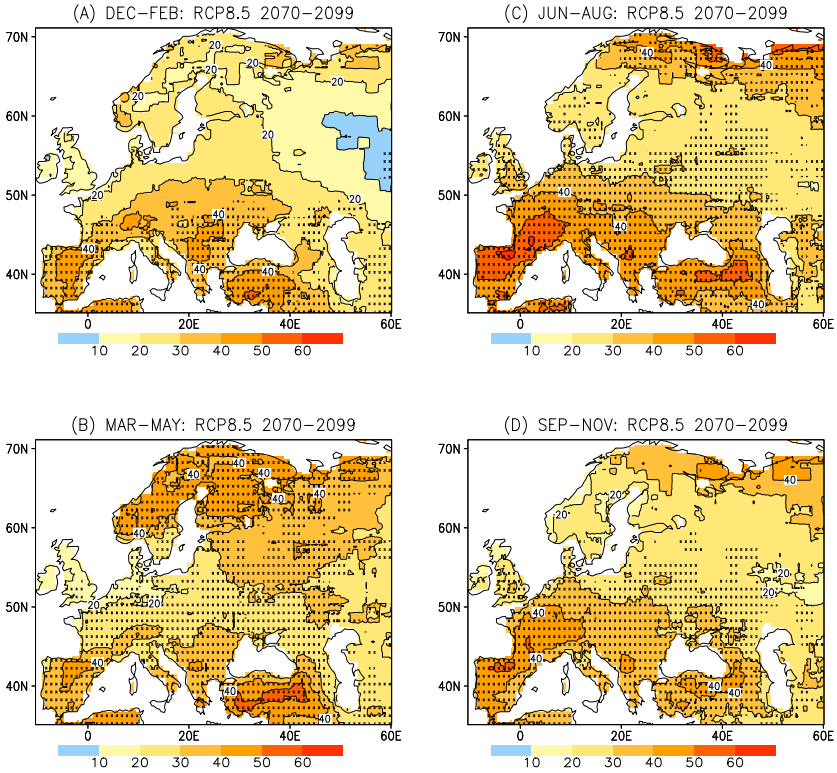

Fig. 8 Multi-model mean relative frequencies (in per cent) of months with an anomalously low soil moisture (such that occurs less frequently than once in 10 years in the simulations for the period 1961–2005) in (a) December-February, (b) March-May, (c) June-August and (d) September-November for the period 2070–2099 under RCP8.5. Areas where at least 23 models out of 26 agree on an increasing frequency of anomalously low soil moisture events (i.e., $p \geq 10\%$) are stippled.

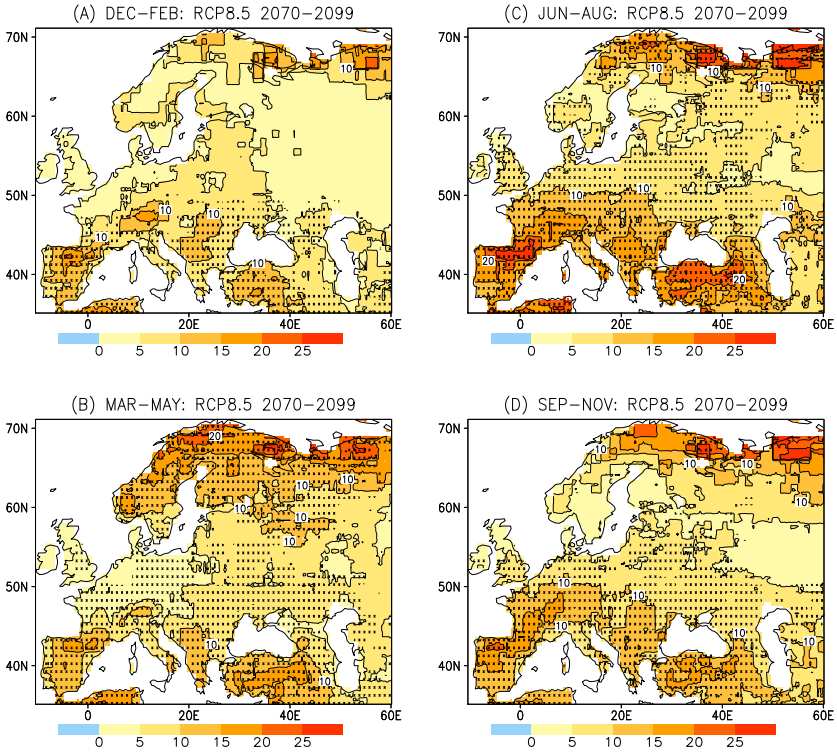

Fig. 9 Multi-model mean relative frequencies (in per cent) of months with an extremely low soil moisture (moisture content lower than the absolute minimum value for that month during 1961–2005) in (a) December-February, (b) March-May, (c) June-August and (d) September-November for the period 2070–2099 under RCP8.5. Areas where 23 models or more simulate a non-zero frequency for such unprecedentedly dry months are stippled.